HOT ELECTRON PRODUCTION, ANOMALOUS ABSORPTION AND EFFECT OF INTENSE ELECTROMAGNETIC FIELDS ON INVERSE BREMSSTRAHLUNG ABSORPTION NEAR THE ELECTRON PLASMA FREQUENCY*

J. H. Brownell, H. Dreicer, R. F. Ellis,† J. C. Ingraham
Los Alamos Scientific Laboratory
Los Alamos, New Mexico 87544

MASTER

ABSTRACT

Measurements are presented of anomalously large microwave absorption near the electron plasma frequency ω_p by a completely ionized plasma. The threshold electric field required for the onset of anomalous absorption has been measured over a range of density that is large enough to clearly separate the effects of Landau-and collisional-damping. Good agreement is demonstrated between these measurements and the threshold values predicted by computer solution of the exact dispersion relation for AC parametric instabilities. Energy distribution measurements are presented for the hot nonthermal electron tail produced by such anomalous absorption. The nature of these distributions depends strongly upon $(\omega_p/\omega)^2$ and microwave power. In some cases a large fraction of the anomalously absorbed power goes into less than 1% of the electrons and a bump develops on the hot tail.

Below the threshold for anomalous absorption we have deduced the classical electron-ion collision rate, ν_{ei}, from a measurement of the inverse bremsstrahlung absorption rate. We report the first experimental evidence that intense electromagnetic fields modify ν_{ei}. Our observations yield a simple empirical relation that applies for AC drift speeds as large as $eE/(m\omega) \approx (kT_e/m)^{1/2}$. Ohmic heating is minimized in these experiments by use of very short microwave pulses.

---

* Work performed under the auspices of the United States Atomic Energy Commission

† Present address: Dept. of Physics, Dartmouth College, Hanover, N.H. 03755

HOT ELECTRON PRODUCTION, ANOMALOUS ABSORPTION AND EFFECT OF INTENSE ELECTROMAGNETIC FIELDS ON INVERSE BREMSSTRAHLUNG ABSORPTION NEAR THE ELECTRON PLASMA FREQUENCY

J. H. Brownell, H. Dreicer, R. F. Ellis†, J. C. Ingraham
Los Alamos Scientific Laboratory
Los Alamos, New Mexico 87544

1. Hot Electrons and Anomalous Absorption

The physics of intense wave propagation in high temperature plasmas involves some processes that are common to many controlled thermonuclear plasma experiments. For example in programs as different as lower hybrid Tokamak heating, relativistic electron beam heating, and laser heating of dense plasmas one encounters the phenomenon of anomalous absorption by the parametric decay of plasma waves or electromagnetic waves. The need for a detailed understanding of this decay process is especially apparent in the program to compress and heat dense DT pellet plasmas with intense laser light. A prerequisite for the success of this important approach is the efficient anomalous absorption of laser light in the ablation plasma where the density is smaller than the critical density (defined by equality between the laser light frequency ω and the electron plasma frequency ω_p). Success is also conditional on the manner in which absorbed energy is distributed among the electrons since energy absorption by too small a fraction of the electrons would result in a hot nonthermal electron tail that could hinder attainment of fusion reactor conditions.[1] Detailed understanding is therefore required about the relationship between anomalous absorption by parametric decay and the resulting heated velocity distribution. Moreover detailed information is required about the dependence of the threshold of the decay process on plasma density. The results of our plasma physics experiments devoted to these questions are detailed below. They can be used to verify the validity of theoretical models and predictions and to suggest theoretical extensions vitally needed at the present time.

1.1 Experimental Techniques

We have studied anomalous heating [2,3] on a well-controlled low density plasma subjected to short microwave pulses. Figure 1(a) shows the experimental setup. The potassium plasma column of a single-ended Q machine ($n \approx 5 \times 10^{10}$ cm^{-3}, $T_e \approx T_i \approx 0.2$ eV) is subjected to the electric field E of a 2-GHz, TM 010 mode microwave resonator (R) with E parallel to the

magnetic field B. A Langmuir probe (LP) measures the radial profile of ion saturation current (I_+) and the radial profile and energy distribution of the hot electrons that stream from R along B during anomalous absorption. The cold collector (CC) is used to energy-analyze hot electrons with energies greater than 2 eV [collection of ambient ($T \approx 0.2$ eV) electrons masks hot-electron collection below 2 eV]. All such hot electrons stream from R to the right without collisions, allowing absolute measurement at CC of their density and power. Using I_+, the microwave absorption rate and n are unfolded, respectively, from the decrease in resonator Q and the resonator frequency shift, due to plasma. Fast microwave switching allows R to be excited repetitively for short time intervals (0.2 to 30 μsec) that minimize microwave perturbation of the plasma equilibrium. Figure 1(b) shows the transmitted power P_T and the hot-electron current I_{HOT} collected at CC as a function of time. Pump depletion in P_T at about 5 μsec indicates anomalous absorption onset, and a reasonable steady state is obtained in P_T and I_{HOT} thereafter. The Q value of R during the steady-state excitation period is determined from the initial P_T decay rate following rapid termination of the incident power.

1.2 Anomalous Absorption Threshold Measurements

For each plasma density there exists a threshold electric field E_c above which we observe (1) a decrease in the Q value of R indicating anomalous absorption onset; (2) hot-electron current at CC; and (3) pump depletion in P_T. E_c measurements as a function of ω_{pp}^2/ω^2 are given in Fig. 2 (black dots) with $v_E = eE_c/m\omega$ and $v_T = (2kT_e/m)^{1/2}$ The observations are independent of the applied magnetic field B over the range 4 KG <B< 10 KG used in the experiment. Microwave pulse lengths used were long enough to permit the instability to grow and short enough to minimize electron heating.

1.3 Threshold Theory for AC Parametric Instabilities

The measured electric field threshold has been compared with the threshold predicted by the computer solution of the exact dispersion relation for AC parametric instabilities. Our computations utilize the Marder and Freidberg numerical formulation for an infinite uniform plasma including electron-ion encounters [4], and modified to include the obliquely propagating electron plasma waves that exist when the electrons are line-tied by a strong applied magnetic field. (We ignore the effect of the magnetic field on ion motion.) In the absence of the externally applied electric field, the frequency of these obliquely propagating waves is

$$\omega \simeq \omega_p \cos\theta \left[1 + \frac{3}{2} k^2 \lambda_D^2\right] \; ; \; \lambda_D = \text{Debye length}$$

where θ is the angle subtended by the wave vector k and B. By including these oblique waves we automatically also describe some features of a constant density finite radius magnetized plasma column which acts like a waveguide for oblique waves, and is similar to the plasma profile in our experiment (I_+ in Fig. 1c).

The numerical results (solid and dashed line in Fig. 2), accurately computed for arbitrary values of the applied electric field, are in good agreement with our observations over the range $0.3 \leq (\omega_{po}/\omega)^2 \leq 1.4$ studied in the experiment without introduction of any arbitrary parameters. At the lower densities $(\omega_{po}/\omega)^2 \lesssim 0.9$ Landau damping is responsible for the sharp increase in threshold field. Collisional damping exceeds Landau damping for $(\omega_{po}/\omega)^2 \gtrsim 0.9$ and determines the threshold in this region. The electron-ion collision rate, ν_{ei}, measured by us on this plasma (See Section 2) was used to introduce the collisional damping rate into the theory. For $(\omega_{po}/\omega)^2 \leq 1$ the lowest threshold is associated with $\theta = 0$ waves while for $(\omega_{po}/\omega)^2 \leq 1$ we can associate the observed minimum threshold with obliquely propagating waves whose angle of propagation is given by $\theta \simeq \cos^{-1}(\omega/\omega_{po})$.

1.4 Anomalous Absorption Rate

The measured microwave absorption rate increases sharply just above threshold (See Fig. 3) and assumes values that are 10 to 20 times the classical value due to electron-ion encounters for ratios of electro-magnetic field intensity to threshold intensity, E^2/E_c^2, of 10 to 40. The determination of the effective collision rate, ν_{eff} is complicated by the need to know the detailed radial distribution of anomalous absorption while the microwave technique only yields the total absorption over the plasma. In the analysis leading to Fig. 3 we have used our measurement of the radial distribution of very hot electrons for this purpose (See Fig. 1c). This ignores the radial distribution of anomalous heating in the body of the electron energy distribution because too little is known about this. Figure 3 also ignores changes in ν_{ei} and in E_c, the threshold electric field, as a result of the small amount of heating which accompanies the pulsed absorption measurement. These corrections are not expected to alter the magnitude of ν_{eff} significantly.

1.5 Anomalously Heated Electron Energy Distributions

Retarding potential probe measurements of F(E) have yielded the first quantitative data (Fig. 4) which show that long tails of hot electrons are produced when the parametric instabilities are driven into their non-linear regimes. The result indicates that the number and distribution of hot electrons is a very sensitive function of ω_p^2/ω^2 and pump power, and may involve the production of a bump on the tail. Some heating of the main body of the electron distribution has also been observed. The sensitive dependence of hot electron properties upon plasma density may be summarized as follows: Two regions of plasma density are found, corresponding to strikingly different properties of the hot electrons: $0.70 \leq \omega_{po}^2/\omega^2 \leq 0.85$, where Landau damping dominates the threshold; and $0.9 \leq \omega_{po}^2/\omega^2 \leq 1.0$, where collisional damping dominates the threshold. Figure 4 displays F(E) curves for a density in each of these regions, with $P = E^2/E_c^2$ as a parameter. The common features for the two cases in Fig. 4 are the following: (1) n_{HOT}/n, the ratio of hot to ambient electron density, increases strongly with increasing P, but is always less than 1% (See Table I); (2) at the lowest P values F(E) is Maxwellian, but at a much higher temperature than ambient; and (3) the average energy U_{av} of the hot electrons increases linearly with $\sqrt{P}$. The

features not in common are these: (1) U_{av} of the hot electrons for the collision-damped region is considerably higher than for the Landau-damped region; (2) the slope of U_{av} versus $\sqrt{P}$ is different for the two regions; and (3) a bump develops in F(E) at higher P values only for densities in the collision-damped region. The sudden change of U_{av} between these two density regions correlates with the expected behavior for electrons moving at the theoretically-predicted phase velocity of the most unstable electron wave, suggesting that wave-particle interactions play an important role. For example, at $\omega_{po}^2/\omega^2 = 0.77$ this energy is 1.6 eV, at $\omega_{po}^2/\omega^2 = 0.94$ it is 5.0 eV, and at $\omega_{po}^2/\omega^2 = 0.96$ it is 7.7 eV. Note that the position of the bump in F(E) at $\omega_{po}^2/\omega^2 = 0.94$ is also consistent with these energies, and that such bumps could also exist at $\omega_{po}^2/\omega^2 = 0.77$ but be at energies too low to be measured by our detector. Another distinction between the two density regions is in the fraction of the measured anomalously absorbed microwave power P_{ANOM} carried by the hot electrons. The absolute power in hot electrons P_{HOT} is computed from F(E). P_{HOT}/P_{ANOM} and n_{HOT}/n are given in Table I for the cases shown in Fig. 4. Only in the collision-damped region, and for higher P values, is a very large fraction of P_{ANOM} given to a very small fraction n_{HOT}/n of the electrons. The estimated uncertainty of P_{HOT}/P_{ANOM} is $\pm$ 50%. Preliminary measurements of the temperature increase of the body of the electron distribution show that a significant fraction of the unaccounted-for P_{ANOM} goes into moderate body heating rather than hot-tail production. Some uncertainty remains in the energy scale of Fig. 4 due to the small change in plasma potential when electrons are heated. This question is still under investigation.

2. Influence of Intense AC Electric Fields on the Electron-Ion Collision Rate in a Plasma

Current interest in the heating of several plasma configurations [5,6] to thermonuclear temperatures centers on efficient absorption of electromagnetic energy by plasma particles. In these cases the time dependent absorption goes hand-in-hand with other important transport processes like heat flow and electron-ion energy equilibration. Although such particle heating is well-known to influence other classical transport processes indirectly through their temperature dependence, it is generally not recognized that the application of intense electromagnetic heating fields may also directly modify classical transport parameters on a time scale that is much shorter than the heating time, without generating plasma instabilities. This effect arises when the electromagnetic field is intense enough to produce significant modifications in the hyperbolic orbits traversed during Coulomb encounters and thus occurs as soon as these fields turn on. Several theoretical treatments [7,8] predict such an orbit modification-electric field effect for the classical AC electrical resistivity or, equivalently, the classical inverse bremsstrahlung absorption rate.[9,10] Our measurements of inverse bremsstrahlung absorption, detailed below, have yielded the first experimental observation of this effect in the form of an electric field dependent electron-ion momentum transfer collision rate.

2.1 Experimental Technique

Using the experimental set-up shown in Fig. 1a we measure the change in

Q due to plasma, expressed as

$$\Delta(1/Q) = \int \left[\frac{\omega_{p_o}^2 \cdot n(r)}{\omega^2 n(o)}\right] \left[\frac{\nu_{ei}(E,T)n(r)}{\omega\, n(o)}\right] E^2 dv \Big/ \int E^2 dV \quad .$$

Here ω_{po} is the electron plasma frequency at r = 0, E is the microwave electric field, and $\nu_{ei}(E,T)$ is the electric field and temperature dependent electron-ion momentum transfer collision rate at r = 0. Equation 1 applies when $\nu_{ei} \ll \omega$, and E parallel to B, two situations that prevail in our experiment. Measurements of $\Delta(1/Q)$ are made as a function of the two most relevant parameters accessible in our experiment. These are the microwave pulse length τ and microwave electric field strength E which play the following roles: Electric Field. E displaces the plasma electrons to the oscillation amplitude $\delta = eE/(m\omega^2) = v_E/\omega$ which may also be expressed as $\delta = \sqrt{2}\, \lambda_D\, (v_E/v_T)\, (\omega_p/\omega)$. Consideration of Debye-shielded binary encounter dynamics suggests that modifications in ν_{ei} will be produced if δ exceeds $\sim 0.1\, \lambda_D$ during the typical electron-ion encounter duration $1/\omega_p$. These requirements are satisfied by $v_E/v_T \gtrsim 0.1$. Pulse Length. The need to separate the effect of Ohmic heating (i.e., temperature changes) on $\nu_{ei}(E,T)$ from the orbit modification effect dictates the use of short pulse lengths. In weak electric fields, with heat conduction ignored, Ohmic heating raises the electron temperature T at the rate

$$\nu_h \equiv \frac{1}{T}\frac{dT}{dt} = \frac{2}{3}\frac{v_E}{v_T}\,\nu_{ei}\,(0,T)$$

where $\nu_{ei}\,(0,T)$ is a function of ω/ω_p. [11] Near $\omega = \omega_p$ we have $\nu_{ei}\,(0,T) = 4\sqrt{\pi}\, n\, Z\, e^4\, \ell n\Lambda/[3\sqrt{2m}(kT)^{3/2}]$. Use of microwave measuring pulses whose duration τ exceeds $1/\nu_h$, might therefore produce temporal changes in ν_{ei} that could mask the more fundamental orbit modification effect. For the purpose of this experiment $\Delta(1/Q)$ is therefore measured with microwave pulses whose $\tau \ll 1/\nu_h$. The duration required for the measurement of Q is 0.1 μsec which is about 0.3 to 0.5 of τ.

Orbit modification may also be masked by anomalous absorption, which causes a marked decrease in resonator Q when E is large enough to excite AC parametric instabilities during the time τ. The threshold for these instabilities measured by us on the same plasma with a $\tau \approx 5$ μsec is shown in Fig. 2. Even though instability growth rate limitations cause the apparent threshold to increase as τ is shortened, the threshold for $\tau \approx 5$ μsec serves as the most conservative boundary for a clear separation of effects. The foregoing considerations led us to study the range $0.55 < (\omega_{po}/\omega)^2 \lesssim 0.65$ where the density is still large enough to give measurable classical absorption below threshold, and yet the density is not so large as to preclude a reasonable search range in v_E/v_T without exceeding the threshold at $v_E/v_T \simeq 0.75$.

2.2 Experimental Observations

Figure 5 shows the values of $\langle\nu_{ei}\rangle$ (dots clustered about dashed line) measured as a function of E or v_E/v_T. The brackets on ν_{ei} indicate that it is the value determined from the measured Q. The normalization $\nu_{ei}(T_o)$ is the value of ν_{ei} deduced from $\Delta(1/Q)$ measurements at $v_E/v_T = 0.0035$. (In such a weak field Ohmic heating is absent for the pulse lengths used and, as shown in Fig. 6, the theoretical value of $\Delta(1/Q)$ (solid line), based upon the local application of $\nu_{ei}(0,T)$ [11] to our trapezoidal density profile, is in excellent agreement with our observed $\Delta(1/Q)$ (dots) for a wide range of $(\omega_{po}/\omega)^2$ at the measured hot plate temperature $T_o = 2250°K$.) For the smallest field shown, E = 10 volts/cm ($v_E/v_T = 0.06$), we find $\langle\nu_{ei}(E,T)\rangle/\nu_{ei}(T_o) \approx 1.0$ as expected. As E increases to E = 150 volts-cm^{-1} ($v_E/v_T = 0.74$), $\langle\nu_{ei}(E,T)\rangle/\nu_{ei}(T_o)$ falls to about 0.4. In such strong fields there is a small increase in T/T_o due to Ohmic heating even for the short pulses used by us. We determine this increase from a computer solution of the energy equation

$$\frac{3}{2} nk \frac{\partial T}{\partial t} - \frac{\partial}{\partial x}\left(K_o(T)\frac{\partial T}{\partial x}\right) = \frac{\omega_p^2\,\nu_{ei}(E,T)}{\omega^2 + \nu_{ei}^2(0,T)} \frac{E^2(x,t)}{8\pi}$$

which is valid during the relatively long period (> 0.1 msec) after application of the microwave pulse before ion response motions manifest themselves in our experiment. The classical thermal conductivity $K_o(T) = 0.96\,k\,(kT)^{5/2}/(\sqrt{m}\,e^4\,\ell n\Lambda)$ without orbit modification was used in this calculation. Orbit modification of $K_o(T)$ would have increased the heat flow only over the 5-7% plasma length occupied by the microwave resonator, and would have resulted in an even smaller computed temperature increase.

We assume $\nu_{ei}(E,T) = \alpha(E)\,\nu_{ei}(0,T)$, and compute T and $\alpha(E)$ from our observed value of ν_{ei} by utilizing Eq. 3 in an iterative computational procedure based on $\alpha^{(n)}(E) = [\nu_{ei}(E,T)/\nu_{ei}(T_o)]\,(T^{(n)}/T_o)^{3/2}$ This scheme converges adequately for n = 3 or 4 and results in the $\alpha(E)$ curve shown in Fig. 5. The dashed line in this figure provided the starting values for the iteration. In agreement with separate Langmuir probe measurements made by us we find the temperature correction to be small and this supports the evidence that the orbit modification effect has indeed been observed with $\alpha(E) < 1$. In the range $0 \le E \le 150$ v-cm^{-1}, the empirical relation $\alpha(E) = (1 + 2\,v_E^2/v_T^2)^{3/2}$, which is obtained by substituting $KT + mv_E^2$ for KT in $\nu_{ei}(0,T)$, is in good agreement with the $\alpha(E)$ values deduced from the measurements. The $\alpha(E)$ values computed by Salat and Kaw [7] in the absence of magnetic field are shown in Fig. 5 for comparison. Their predicted $1 - \alpha$ values are only 10-30% of our observed $1 - \alpha$. A recent numerical reevaluation of the Salat and Kaw result by Wright [12] reduces this difference somewhat, but still leaves a very significant discrepancy between theory and experiment. Although we have observed no dependence of $\nu_{ei}(0,T)$ on magnetic field we have not yet experimentally ruled out the possibility that a dependence of α on B can explain this discrepancy.

We have observed an electric field dependent electron-ion collision rate for $v_E/v_T \leq 0.74$ by carefully avoiding masking effects due to Ohmic heating and AC parametric instabilities (for $v_E/v_T > 0.74$ this electric field effect is expected to become even stronger). Our observations have application to all classical transport processes produced by electron-ion encounters in the presence of intense electromagnetic fields. In particular we conclude that the application of intense electromagnetic heating fields to a long magnetized plasma column [6] could significantly reduce absorption and equilibration rates and could significantly increase the electron thermal conduction loss to the column ends compared to the generally accepted values that apply only in the absence of an electromagnetic field. In the case of the laser illuminated DT pellet experiment [5], increased heat flow could occur in the pellet's low density plasma ablation cloud, and this would reduce the requirements for symmetric laser illumination imposed by the need for a high compression spherical implosion [13].

REFERENCES

[1] J. S. Clark, H. N. Fisher, and R. J. Mason, Phys. Rev. Lett. 30, 89 (1973); J. Nuckolls, L. Wood, R. Thiessen, and G. Zimmerman, Lawrence Livermore Laboratory, University of California Report No. UCRL-50021-72-1 (unpublished), p. 102.

[2] H. Dreicer, D. B. Henderson, and J. C. Ingraham, Phys. Rev. Lett, 26, 1616 (1971).

[3] H. Dreicer, R. F. Ellis, and J. C. Ingraham, Phys. Rev. Lett. 31, 426 (1973).

[4] J. P. Freidberg and B. M. Marder, Phys. Rev. A 4, 1549 (1971), and private communication 1971.

[5] J. S. Clark, H. N. Fisher, and R. J. Mason, Phys Rev. Lett 30, 89 (1973).

[6] J. M. Dawson, A. Hertzberg, R. E. Kidder, G. C. Vlases, H. G. Ahlstrom and L. C. Steinhauer, Proceedings of the Fourth International Conference on Plasma Physics and Controlled Nuclear Fusion Research 1, 673 (Madison 1971).

[7] A. Salat and P. K. Kaw, Phys Fluids 12, 342 (1969); T. P. Wright, Bull. Am. Phys. Soc. 18, 1303 (1973).

[8] V. P. Silin, Zh Eksper, Teor. Fiz 47,2254 (1965) Sov. Phys.-JETP 20, 1510 (1965).

[9] S. Rand, Phys Rev. 136, B231 (1964); G. J. Pert, J. Phys A: Gen. Phys. 5, 1506 (1972); G. J. Pert, J. Phys A: Gen. Phys. 5, 1221 (1972).

[10] H. A. Bethe, Los Alamos Report LA-5031-MS (1972).

[11] J. Dawson and C. Oberman, Phys Fluids 5, 517 (1962).

[12] T. P. Wright private communication 1974.

[13] D. B. Henderson and R. L. Morse, Phys Rev Lett. 32, 355 (1974).

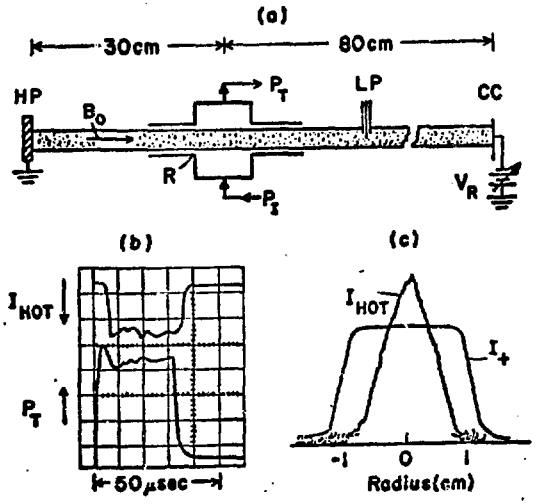

Fig. 1 (a) Experimental setup; (b) hot-electron current I_{HOT} collected at CC, and transmitted power P_T; (c) radial profile of I_{HOT} and of ion saturation current I_+, as measured by LP.

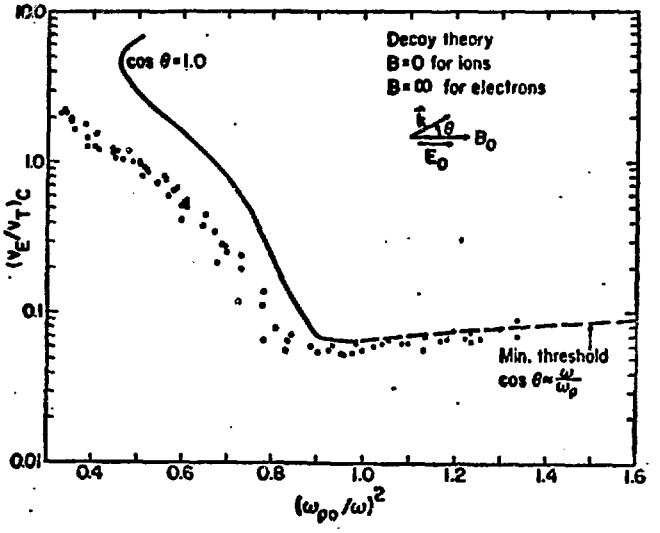

Fig. 2 Threshold field vs. $(\omega_{po}/\omega)^2$

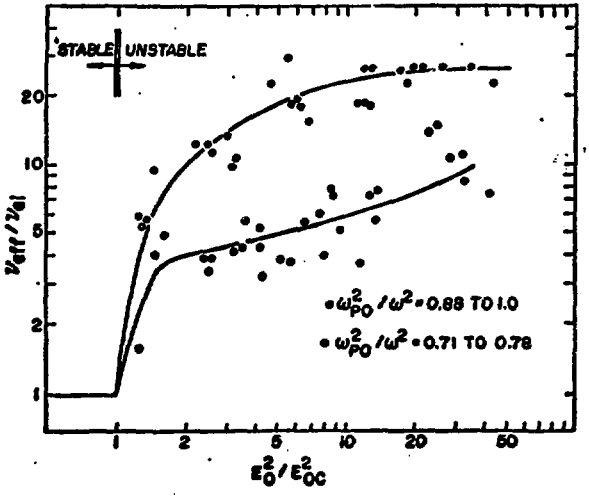

Fig. 3 Normalized effective collision rate vs. $(E/E_c)^2$

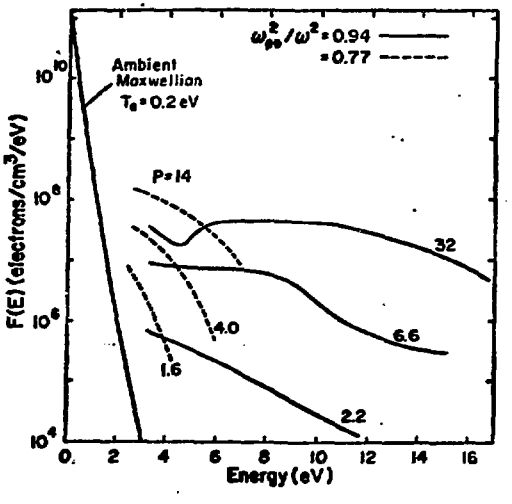

Fig. 4 Hot electron distributions as a function of energy with P and $(\omega_{po}/\omega)^2$ as parameters compared with ambient Maxwellian.

TABLE I. Hot-Electron Properties

ω_{po}^2/ω^2	P	$10^2 n_{HOT}/n_o$	P_{HOT}/P_{ANOM}
	1.6	0.015	0.021
0.77	4.0	0.10	0.10
	14.	0.75	0.13
	2.2	0.0038	0.12
0.94	6.6	0.096	0.80
	32.	0.77	1.10

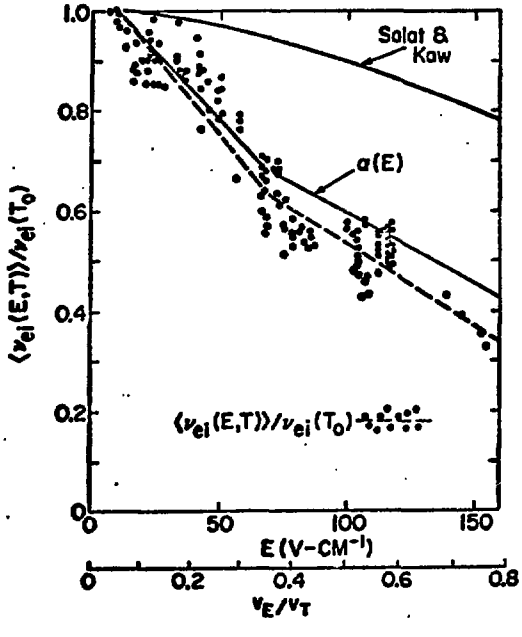

Fig. 5 Electric field dependent collision rate vs. electric field or v_E/v_T

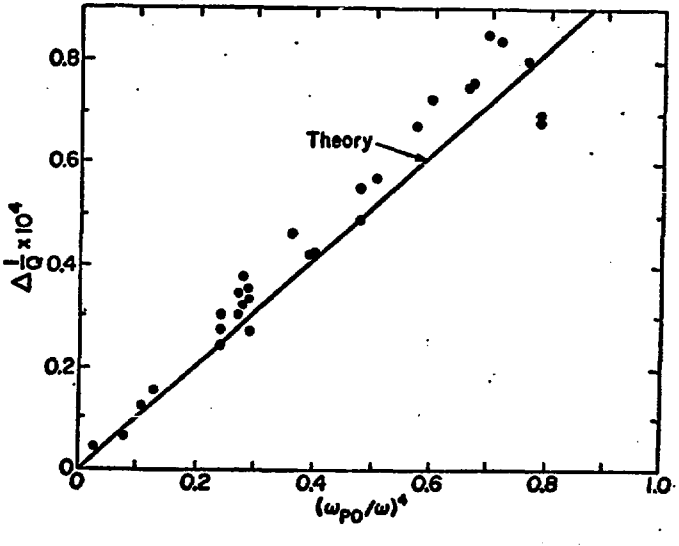

Fig. 6 $\Delta(1/Q)$ vs. $(\omega_{po}/\omega)^4$ for $v_E/v_T = 0.0035$

TABLE I. Hot-Electron Properties

ω_{po}^2/ω^2	P	$10^2 n_{HOT}/n$	P_{HOT}/P_{ANOM}
	1.6	0.015	0.021
0.77	4.0	0.10	0.10
	14.	0.75	0.13
	2.2	0.0038	0.12
0.94	6.6	0.096	0.80
	32.	0.77	1.10